Sensitivity of the solar resource in solar tower plants to aerosols and water vapor

Cite as: AIP Conference Proceedings **2126**, 190006 (2019); https://doi.org/10.1063/1.5117703
Published Online: 26 July 2019

Thierry Elias, Didier Ramon, Jean-Florian Brau, and Mustapha Moulana

Sensitivity of the Solar Resource in Solar Tower Plants to Aerosols and Water Vapor

Thierry Elias[1, a)], Didier Ramon[1], Jean-Florian Brau[2], Mustapha Moulana[1]

[1] *HYGEOS, Euratechnologies, 165 av. de Bretagne, 59000 Lille, France*
[2] *EDF R&D, 6 Quai Watier, 78400 Chatou, France*

a) Corresponding author: te@hygeos.com

Abstract. We make a sensitivity study of the solar resource in a solar tower plant, to aerosols, water vapour and solar position, considering typical atmospheric conditions observed at Ouarzazate, Morocco. Four solar resource parameters were defined: the direct normal irradiance (DNI), incident at the heliosat, the slant path attenuation between the heliostats and the receiver (A_{sp}), the solar irradiance incident at the receiver (SIR), and the solar irradiance lost between the heliostat and the receiver (SIR_{loss}). The aerosol optical thickness (AOT), which varies strongly from winter to summer at Ouarzazate, is the main factor on *DNI* and A_{sp}. However, despite a factor of 10 in *AOT* between typical winter and summer conditions, A_{sp} varies by a factor of only 2.7 and SIR_{loss} by a factor of only 1.9, for two reasons: 1) the aerosol layer height (ALH) is correlated to *AOT* and has an opposite effect on A_{sp}; 2) *DNI* and A_{sp} are anti-correlated. Consequently, despite 100% standard deviation on *AOT* observed during 2012, the relative standard deviation of A_{sp} is only 60%, and only 47% for SIR_{loss}. Consequently, to estimate solar resource in a solar tower plant, it is recommended to compute directly *SIR* and not combining *DNI* and A_{sp} derived from different sources. Also, it is recommended to make computations by considering observed variability of most atmospheric parameters at high time resolution. Computing the solar resource with the annual average of *ALH* instead of its seasonally dependent value generates an over estimation of A_{sp} from 5.9% to 6.2%. With the annual average of *AOT* or the Ångström exponent instead of the hourly-varying values, *SIR* is changed by ±3%.

INTRODUCTION

Solar resource in solar plants needs to be estimated because of the large variability of several atmospheric parameters in time and space. Two solar resource parameters are generally required in solar tower plants (STPs), which are 1) the direct normal irradiance (DNI) depending on atmospheric scattering and absorption, and 2) the slant path attenuation (A_{sp}) between the heliostats and the receiver. A_{sp}, which is identified as one of the optical losses in STPs by Li *et al.* [1], could result in a reduction of the annual yield larger than 10% in a typical STP [2].

DNI and A_{sp} were mostly studied separately [e.g. 3, 4, 5] while they can be strongly (anti-)correlated. We consequently propose a unique sensitivity study of all solar resource parameters: not only *DNI* and A_{sp}, but also of the solar irradiance incident at the receiver (SIR), and of the solar irradiance lost between the heliostat and the receiver (SIR_{loss}). Moreover, we do not only consider variability in the aerosol optical thickness (AOT) [e.g. 2], but also in the Ångström exponent (aerosol size indicator), the aerosol layer height (ALH), and the water vapor content in the atmosphere (WVC). It is indeed important to consider simultaneous changes in several atmospheric parameters, as some can be correlated. For example at Ouarzazate (Morocco), nearby the Noor STP projects, *ALH* is correlated with *AOT*, both increasing from winter to summer, with an expected reduced impact on A_{sp} [4]. We also consider the influence of the solar zenith angle (SZA) [5]. Observations made by the aerosol robotic network (AERONET) [6] indicate the potential range of variability of the atmospheric parameters, and reanalysis data by the European Center for Medium Weather Forecasts (ECMWF) indicate the variability in the vertical distribution of aerosols. The solar resource parameters are computed for realistic winter and summer conditions at Ouarzazate. Following the recommendations to use the finest time resolution [2], computations are made at the hourly time scale.

SolarPACES 2018
AIP Conf. Proc. 2126, 190006-1–190006-10; https://doi.org/10.1063/1.5117703
Published by AIP Publishing. 978-0-7354-1866-0/$30.00

Section 2 describes the methodology and Section 3 the atmospheric properties observed at Ouarzazate by AERONET. Results are commented in Sections 4 and 5. Section 4 shows the sensitivity study by defining typical conditions at Ouarzazate, and in Section 5 the impact of the full variability in input parameters is studied by applying the algorithm on observations made at Ouarzazate in 2012, at 1-hour resolution.

METHODOLOGY

The Four Solar Resource Parameters

The solar irradiance incident at the receiver (SIR) of a STP is:

$$SIR = F_{ESD} \int_{250nm}^{4000nm} E_{sun}(\lambda) T_{col}(SZA, \lambda) T_{surf}(SPA, DHR, \lambda) d\lambda \quad (1)$$

F_{ESD} is the Earth-Sun distance correcting factor, $E_{Sun}(\lambda)$ is the extra-terrestrial solar irradiance at the wavelength λ, $T_{col}(SZA,\lambda)$ is the atmospheric column transmittance along the solar zenith angle (SZA), and $T_{surf}(SPA,DHR,\lambda)$ is the slant path transmittance along the slant path angle (SPA). The slant path transmittance also depends on the heliostat-receiver distance (DHR). The heliostat reflectance is considered equal to 1 at all wavelengths. The slant path transmittance (T_{sp}) in the broadband solar spectrum can be defined in function of *SIR* and *DNI* [5, 7] as:

$$T_{sp} = SIR / DNI \quad (2)$$

Both *SIR* and *DNI* are defined according to the 'strict' definition given by Blanc *et al.* [8] for the *DNI*. Beams in the only solar direction are counted, and which were not scattered by the atmosphere. Consequently the circumsolar radiation is not accounted for. *DNI* is then expressed as:

$$DNI = F_{ESD} \int_{250nm}^{4000nm} E_{sun}(\lambda) T_{col}(\lambda) d\lambda \quad (3)$$

The slant path attenuation A_{sp} (%) and the solar irradiance lost between the heliostat and the receiver, SIR_{loss}, are computed as:

$$A_{sp} = (1 - T_{sp}) * 100 \quad (4a)$$

$$SIR_{loss} = DNI - SIR = DNI \, . \, A_{sp} / 100 \quad (4b)$$

The four solar resource parameters studied here are *DNI*, *SIR*, A_{sp} and SIR_{loss}. They are defined by the monochromatic transmittance described in next Section.

The Aerosol Vertical Profile Hypothesis

The monochromatic transmittances can be decomposed as:

$$T_{col}(\lambda) = T_{Ray,col}(\lambda) \, . \, T_{gas,col}(\lambda) \, . \, T_{aer,col}(\lambda) \quad (5a)$$

$$T_{surf}(\lambda) = T_{Ray,surf}(\lambda) \, . \, T_{H2O,surf}(\lambda) \, . \, T_{aer,surf}(\lambda) \quad (5b)$$

$T_{Ray,col}(\lambda)$ and $T_{Ray,surf}(\lambda)$ are the transmittances caused by Rayleigh scattering, along the atmospheric column and in the slant path, respectively. $T_{gas,col}(\lambda)$ and $T_{H2O,surf}(\lambda)$ are transmittances caused by absorbing gases. Main variable absorbing gases in the atmospheric column are water vapour and ozone, and only water vapour is considered in the slant path. The monochromatic aerosol transmittance is defined according to the Beer-Lambert-Bouguer law as:

$$T_{aer,col}(\lambda) = e^{-\frac{AOT(\lambda)}{cos(SZA)}} \quad (6a)$$

$T_{aer,surf}(\lambda)$ can be expressed in function of the aerosol optical thickness (AOT) and the aerosol layer height (ALH) within the two hypothesis of a uniform distribution of aerosols and of an exponential decay, both in a single layer of height ALH [7]:

$$T_{aer,surf}(\lambda) = e^{-\frac{AOT(\lambda)\ z_T}{cos(SPA)ALH}} \tag{6b}$$

z_T is the receiver's altitude. Next Section describes how to compute each component.

Radiative Transfer Computations

Monochromatic transmittances, from top of the atmosphere to ground level, and from ground level up to the receiver, are computed according to the Beer-Lambert-Bouguer law (Eq. 6b), and *SIR* and *DNI* are computed according to Eq. 1 and 3. The Rayleigh optical depth is computed according to Bodhaine *et al.* [9], and scaled with the atmospheric pressure. Ozone and NO_2 absorption cross sections are taken from Bogumil *et al.* [10], and for other gases like H_2O, CO_2, CH_4, we used the absorption band parametrization provided by Kato *et al.* [11]. The gas and thermodynamic profiles are adopted from the AFGL US summer standard atmosphere [12]. The extra-terrestrial solar spectrum is taken from Kurucz [13]. Spectral integration is made between 250 and 4000 nm to consider the full solar radiation spectrum.

The water vapour optical thickness computed from the AFGL atmosphere is scaled linearly with the column water vapour content fixed empirically or provided by AERONET. Then the AFGL atmosphere profile is used to derive the proportion of water vapour at surface level. We consider a variable *AOT* spectral dependence, while the empirical models usually computed *DNI* with a constant value of the Ångström exponent [14]. We mix desert dust and continental aerosols as modelled by OPAC [15] to reproduce both *AOT* and the Ångström exponent. The resulting model is used to compute the optical thickness at all wavelengths of the solar spectrum.

As proposed by Elias *et al.* [4, 7], the seasonal changes of *ALH* are modelled by using the boundary layer height (BLH) provided by ECMWF at 15:00 for Ouarzazate. The heliostat-tower distance is 1000 m, and the receiver's height z_T is 200 m. The slant path angle is then 78.7° and the heliostat-receiver distance DHR is 1020 m.

ATMOSPHERIC CONDITIONS AT OUARZAZATE

The input parameters are defined by observations acquired by AERONET at Ouarzazate, Morocco (30.92837° N, 6.91287° W, 1136 m above sea level) in 2012, at the 2.0 quality level. The observation data set extends from 10 February to 31 December 2012. Table 1 gives the annual average and the standard deviation of the atmospheric parameters.

AOT, which can be used as an indicator of the aerosol load in the atmosphere, is usually highly variable in time and space. The annual average of *AOT* was 0.16 at Ouarzazate in 2012. The standard deviation reached 100% of the annual average because of changes in aerosol properties from hourly to monthly resolution. The monthly average of *AOT* was 0.04 in December 2012, January 2014 and ~0.40 in August 2012, 2014 [4].

The annual average of the Ångström exponent indicates a significant presence of large desert dust aerosols. It follows an annual cycle opposite to *AOT*, and the monthly average of the Ångström exponent was 1.30 in December 2012, 0.94 in January 2013, and 0.30 in August 2012. *WVC* follows an annual cycle similar to the Ångström exponent, with a monthly average of 0.4-0.7 g/cm^2 in December 2012-2014, and January 2013-2014, and of 1.2-1.4 g/cm^2 in July-August 2012-2013. The annual average of *SZA* is relatively large because not only noon is considered. According to ECMWF ERA-Interim [16], the monthly average of BLH at 15:00 was 1.3-1.6 km in December 2012-2014, and January 2013-2014, and it was 4.3 km in August 2012-2014.

TABLE 1. Annual average of parameters observed at Ouarzazate in 2012 by AERONET.

Parameter	F_{ESD}	SZA (°)	AOT	Ångström exponent	ALH (km)	WVC (g/cm^2)
Annual average	1.007±0.022	51±20	0.164±0.165	0.72±0.43	3.3±1.0	0.95±0.40
Data source	computation	computation	AERONET	AERONET	ECMWF	AERONET

THE SENSITIVITTY STUDY OF THE SOLAR RESOURCE PARAMETERS

Both ***Figures 1 and 2*** show the dependence of the four solar resource parameters on *AOT*, for different input data sets. First, computations are made for atmospheric conditions observed in average at Ouarzazate in summer by AERONET (red curve in ***Fig. 1 and 2***), i.e. the Ångström exponent is set to 0.3 and the water vapour content to 1.2 g/cm^2 (***Table 2***). According to ERA Interim, *ALH* is set to 4.0 km. Moreover the geometric conditions of 1st August 13:00 UT are considered, with *SZA*=14.7° (optical air mass of 1.03) and F_{ESD}=0.97. Computations are made for the standard atmospheric pressure of 1013.25 hPa. *AOT* varies from 0.04 to 1.00 representing the full range observed at the daily resolution. Second, each parameter is also changed to winter conditions, independently to others which are kept constant. The Ångström exponent is set to 1.0, *WVC* to 0.6 g/cm^2 and *ALH* to 1.3 km (***Table 2***). The geometric conditions are also changed to 1st January 13:00 UT, with *SZA*=54.4° (optical air mass of 1.71). Third, all parameters are changed simultaneously to reproduce the winter conditions. Eventually, 1st August and 1st January are simulated by setting *AOT* to only one value, 0.40 and 0.04 respectively, and F_{ESD} is set to 1.03 on 1st January.

TABLE 2. Input values for each simulation set. Estimated values of solar resource parameters are also given for the '1st January' and the '1st August' simulations, while for other simulations they are shown in Fig. 1 and 2. Bold numbers indicate winter conditions.

		Summer noon	Winter SZA	Winter Ångström exponent	Winter ALH	Winter WVC	Winter noon	1st August noon	1st January noon
Input parameters	F_{ESD}	0.97	0.97	0.97	0.97	0.97	0.97	0.97	**1.03**
	SZA (°)	14.7	**54.4**	14.7	14.7	14.7	**54.4**	14.7	**54.4**
	AOT	0.04-1.0	0.04-1.0	0.04-1.0	0.04-1.0	0.04-1.0	0.04-1.0	0.40	**0.04**
	Ångström	0.3	0.3	**1.0**	0.3	0.3	**1.0**	0.3	**1.0**
	ALH (km)	4.0	4.0	4.0	**1.3**	4.0	**1.3**	4.0	**1.3**
	WVC (g/cm^2)	1.2	1.2	1.2	1.2	**0.6**	**0.6**	1.2	**0.6**
Computed solar resource parameters	DNI (W/m^2)	/	/	/	/	/	/	683	945
	SIR (W/m^2)	/	/	/	/	/	/	607	906
	Asp (%)	/	/	/	/	/	/	11.2	4.2
	SIR_{loss} (W/m^2)	/	/	/	/	/	/	76	40

DNI and SIR

As already shown by other authors, *DNI* is strongly dependent on *AOT* and on *SZA* (***Fig. 1***). *DNI* at noon decreases from 907 to 389 W/m^2 for *AOT* increasing from 0.10 to 1.0, in summer conditions. Similarly Gueymard [17] mentioned a decrease in DNI from 850 to 300 W/m^2 from "relatively clean conditions to dust storm conditions". *DNI* also decreases for increasing *SZA*, by 133 W/m^2 (-15%) for *SZA* of 14.7° to 54.4°, at *AOT*=0.10, and by 197 W/m^2 (-51%) at AOT=1.0.

On the contrary, *DNI* increases for increasing Ångström exponent and decreasing *WVC*. Expectedly, the influence of the Ångström exponent increases with the aerosol contribution, and *DNI* increases by 11 W/m^2 for *AOT*=0.10 but by 64 W/m^2 at *AOT*=1.0 (+1% and +16%, resp.). On the contrary, the *WVC* influence increases for large values of *DNI*, and *DNI* increases by 25 W/m^2 at *AOT*=0.10 and by 12 W/m^2 at *AOT*=1.0 (+3% for both). Expectedly, *DNI* is not affected by *ALH*. Applying all changes simultaneously, the *SZA* influence is partly compensated in winter by both Ångström exponent and *WVC* influences. Consequently, in winter at noon *DNI* decreases by 89 W/m^2 at *AOT*=0.10, relatively to summer conditions, and by 116 W/m^2 at *AOT*=1.0.

The *SIR* sensitivity is similar to the *DNI* sensitivity to *AOT*, the Ångström exponent, *WVC*, and *SZA*. However, *SIR* is also strongly affected by *ALH*. As for the Ångström exponent, the *ALH* influence increases with the aerosol contribution. *SIR* decreases by 41 W/m^2 at *AOT*=0.10 and by 114 W/m^2 at *AOT*=1.0 for *ALH* decreasing by a factor of 3 (-5% and -38%, resp.). Eventually, the seasonal difference is larger in *SIR* than in *DNI*, *SIR* decreasing by 100-140 W/m^2 for *AOT* in the 0.10-1.0 range.

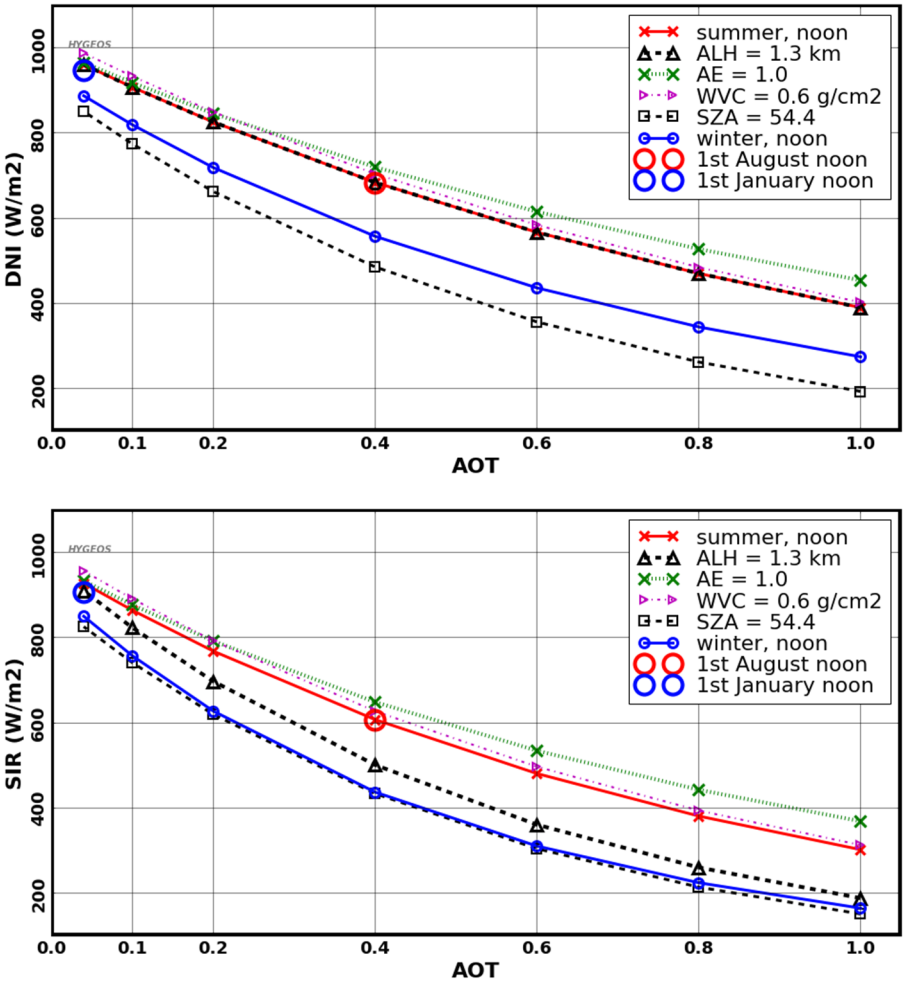

FIGURE 1. Sensitivity of the direct normal irradiance (DNI, top) and the solar irradiance incident at the receiver (SIR, bottom) on solar and atmospheric parameters (see ***Table 2***). Curves are plotted in function of the aerosol optical thickness at 550 nm (AOT), except for 1st August and 1st January noon.

The Slant Path Attenuation and SIR_{loss}

Figure 2 shows the sensitivity of A_{sp} and SIR_{loss}. A_{sp} is strongly dependent on both *AOT* and *ALH*. A_{sp} increases with *AOT*, from 4.8% at *AOT*=0.10 to 22.6% at *AOT*=1.0 (summer conditions). With *ALH* decreasing by a factor of 3, A_{sp} increases to 9.3% at *AOT*=0.10 and from 11.2% to 26.8% at *AOT*=0.40. On the contrary, A_{sp} decreases for increasing Ångström exponent because *SIR* is more affected than *DNI* as the optical pathway is longer for *SIR*. A_{sp} is little affected by the water vapour content [18]. A_{sp} is even affected by *SZA*, as *DNI* and *SIR* both depend on *SZA*, but the influence remains smaller than 1% from 14.7 and 54.4°. Considering all changes simultaneously, the *ALH* influence is partly compensated by other influences, nevertheless the winter influence on A_{sp} remains strong. Indeed A_{sp} increases from 4.8 to 7.6% from summer to winter at *AOT*=0.10, and by a factor of 2 at *AOT*=0.40. Such magnitudes of A_{sp} are significant as a slant path attenuation of 20% could result in power output reduction by 4-12%, according to the plant dimensions and the thermal storage capacities [5].

Similarly to A_{sp}, SIR_{loss} is strongly affected by *AOT* and *ALH*, but also by *SZA* (Fig. 2). SIR_{loss} increases with decreasing *ALH*, while it decreases for increasing *SZA*. For *ALH* decreasing by a factor of 3, SIR_{loss} increases by a factor larger than 2, at *AOT* > 0.10. For *SZA* increasing to 54.4°, SIR_{loss} decreases by 10 W/m^2 at *AOT*=0.10 but by 46 W/m^2 at *AOT*=1.0 (-23% and -52%, resp.). Eventually, SIR_{loss} changes by a factor smaller than ~1.6 from summer to winter. The Ångström exponent has a negligible effect on SIR_{loss}.

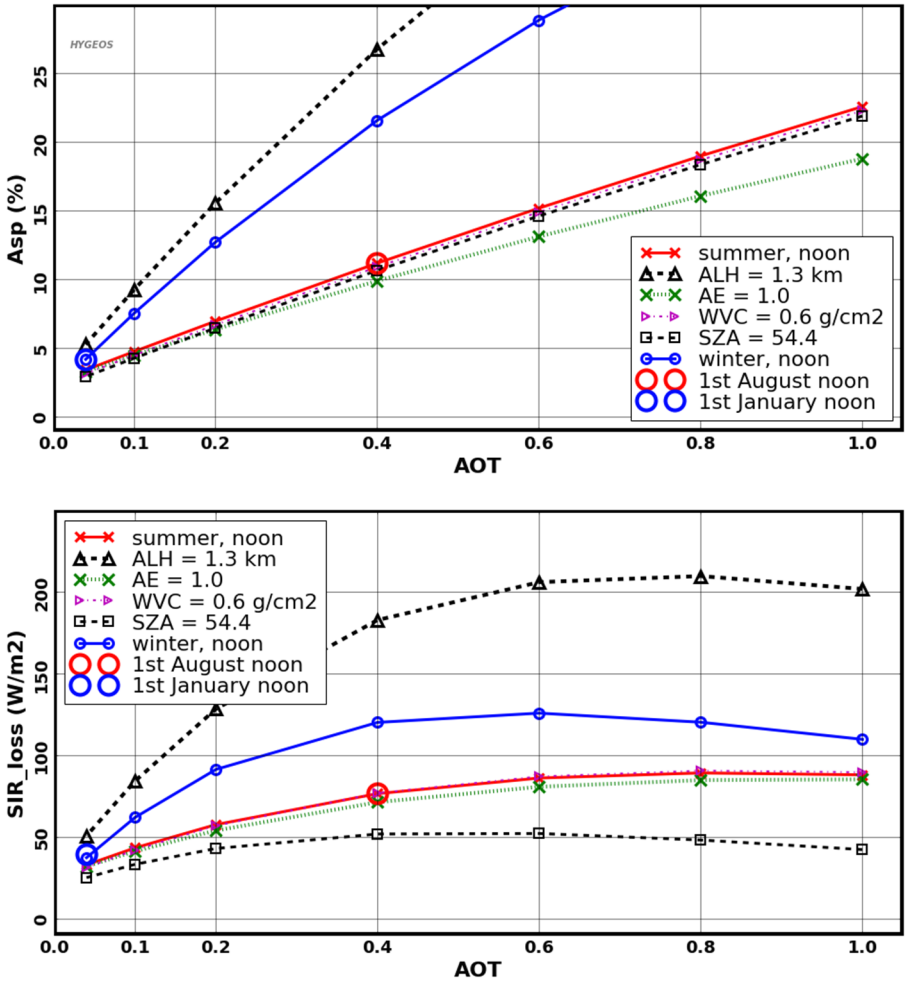

FIGURE 2. As Fig. 1 but for the slant path attenuation (A_{sp}, left) and the solar irradiance lost in the slant path (SIR_{loss}, right).

SIR_{loss} reaches a maximum when *AOT* increases (Fig. 2). For example SIR_{loss} for *ALH*=1.3 km increases from *AOT*=0.04 to *AOT*~0.80 and then slightly decreases for larger *AOT*. This must be caused by saturation of atmospheric extinction at some wavelengths. As it was mentioned for water vapour [18], attenuation at some wavelengths can not increase when the radiation is already completely extinguished. The optical pathway increasing with *SZA*, this saturation effect is stronger with larger *SZA* (and for larger DHR), and for *SZA*=54.4° the SIR_{loss} maximum is reached for *AOT*~0.50. Eventually, the SIR_{loss} maximum of 126 W/m^2 is reached at *AOT*~0.60 in winter, and of 89 W/m^2 at *AOT*~0.90 in summer. Also, it was checked that other AFGL atmospheres have little impact on the water vapour influence in the slant path. In situ measurements may be necessary to better represent the water vapour content in the surface atmospheric layer, or the water vapour layer height [19].

It must be noted that the simulated values of *DNI*, *SIR*, and SIR_{loss} showed in ***Table 2*** and ***Fig. 1***, are biased high compared to time averages because computations are made at noon, when occurs the daily maximum of *DNI*, *SIR*, and even of SIR_{loss}. ***Fig. 3*** shows SIR_{loss} computed for two days at Ouarzazate with different *AOT*, according to AERONET. On both days, SIR_{loss} is close to 0 at ~06:00 UT, increases until 12-13:00, and decreases back. On 30 April 2012 with *AOT*~0.04, SIR_{loss} reached 32 W/m^2 and on 9 August 2012 with *AOT*~0.40 SIR_{loss} reaches 65 W/m^2. In ***Fig. 2***, the minimum value of SIR_{loss} is 35 W/m^2 because it is computed at noon, and ***Fig. 3*** shows that SIR_{loss} could be smaller at other times of the day.

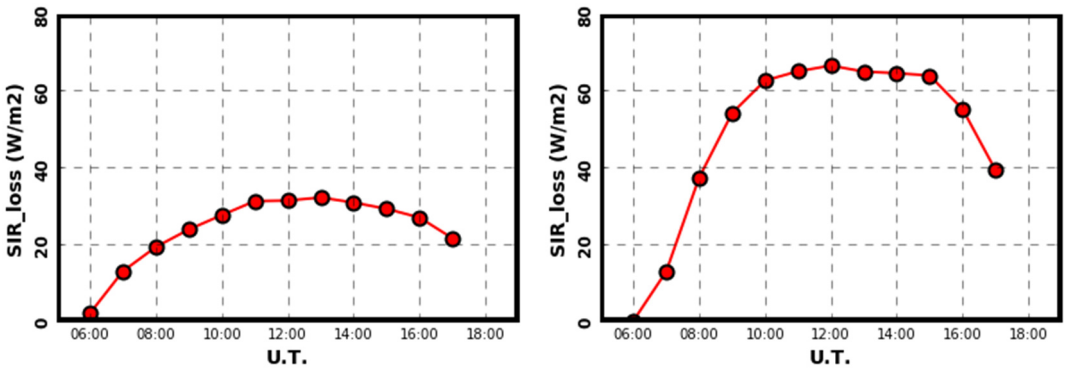

FIGURE 3. SIR_{loss} computed with hourly averages of AERONET data acquired at Ouarzazate on30/04/2012 (left) and on 09/08/2012 (right) when *AOT* was contrasted: *AOT*=0.04 (left) and *AOT*=0.40 (right).

Simulated Seasonal Behaviour of the Solar Resource Parameters at Ouarzazate

While *AOT* changed from 0.04 to 1.0 for summer and winter simulations, *AOT* is set to 0.04 for 1st January and to 0.40 for 1st August (***Table 2***), consistently with observations. Moreover F_{ESD} is set to 1.03 for 1st January while it is 0.97 for 1st August.

For same *AOT*, both *DNI* and *SIR* are larger in summer than in winter because of smaller *SZA* (at noon) (***Fig. 1***). However, as *AOT* is ten times smaller on 1st January than on 1st August, and the Sun is closer to Earth, both *DNI* and *SIR* at noon are eventually larger on 1st January than on 1st August (***Table 2*** and ***Fig. 1***). Mostly because of the *ALH* influence, both A_{sp} and SIR_{loss} are larger in winter than in summer for same *AOT* (***Fig. 2***). But as with *DNI* and *SIR*, the *AOT* change reverses the 1st January - 1st August difference, and A_{sp} and SIR_{loss} become smaller on 1st January than on 1st August (***Table 2*** and ***Fig. 2***). Because F_{ESD} affects both *DNI* and *SIR*, the Earth-Sun distance has no influence on A_{sp}. Eventually, SIR_{loss} on 1st January is smaller by less than a factor of 2 than on 1st August (***Table 2***).

APPLICATION: VARIABILITY OF THE SOLAR RESOURCE ESTIMATE

Section 4 showed the impact on the solar resource estimates of partial correlation both between some input parameters and between solar resource parameters. We now study the impact of the variability of the input parameters, as observed at Ouarzazate in 2012 by AERONET.

Impact of the Input Parameter Variability

The AERONET measurements are averaged over 1 hour, and the solar resource parameters are computed at 1-hour resolution, but with monthly averages of *BLH*. The solar resource parameters are then averaged over the year. The atmospheric pressure is changed to 880 hPa, consistently with Ouarzazate altitude, affecting the Rayleigh scattering, but with a small impact on *DNI*.

According to AERONET, *DNI* was 717±245 W/m^2 at Ouarzazate in 2012 and *SIR* was 679±40 W/m^2 (Table 3). A_{sp} was 5.9±3.5% and SIR_{loss} was 38±18 W/m^2. It can be noted that mean *SIR* was slightly different to the product of mean *DNI* and mean A_{sp}. The product of mean *DNI* and mean A_{sp} also over estimated SIR_{loss} by ~10%. It is consequently important to compute directly *SIR*, instead of separately *DNI* and A_{sp}. Results are consistent with [2] who found 3.1-5.9% reduction in the annual yield performance at Ouarzazate because of the slant path attenuation, according to the solar plant dimensions and thermal storage capacities.

Despite 100% standard deviation on *AOT*, and more than 50% standard deviation on the Ångström exponent and on *WVC*, the standard deviation of A_{sp} was only ~65% and of SIR_{loss} was smaller than 50%. This is consistent with results of Section 4, showing that the variability of A_{sp} is reduced because of compensations between several input parameters. The variability in the atmospheric parameters is changed to understand the origin of the variability of the solar resource parameters. Computations are first made for all input parameters constant (Table 3, data set d1), equal to the annual averages (Table 1). *DNI* significantly increases to 800 W/m^2 (+12%) while A_{sp} remains constant. Consequently *SIR* proportionally increases, and SIR_{loss} reaches 48 W/m^2 (+26%). Both *DNI* and *SIR* are slightly

smaller than the average of 1st January and 1st August (Table 2). Next Section shows what parameter is mostly responsible for the difference between the annual average and the values for constant input parameters.

TABLE 3. Solar resource parameters at Ouarzazate in 2012. Computations are made at 1-hour resolution and averaged over the year. Standard deviations are given in the input parameter rows. In the 3rd column ('reference'), all input parameters are variable at 1-hour resolution, while in the last column (data set d1) all parameters are constant (standard deviation = 0), equal to the annual average (Table 1). In other columns (d2 to d7), one or several input parameters are set constant.

	Parameter	**Reference**	**d4**	**d5**	**d6**	**d7**	**d3**	**d2**	**d1**
Input parameters	F_{ESD}	0.022	0.022	0.022	0.022	0.022	0.022	0.022	0
	SZA (°)	20	20	20	20	20	20	20	0
	AOT	0.165	0	0.165	0.165	0.165	0.165	0	0
	Ångström exponent	0.43	0.43	0	0.43	0.43	0	0	0
	ALH (km)	1.0	1.0	1.0	0	1.0	0	0	0
	WVC (g/cm^2)	0.4	0.4	0.4	0.4	0	0	0	0
Computed solar resource parameters	DNI (W/m^2)	717±245	703±211	735±238	717±245	714±240	732±233	702±209	800
	SIR (W/m^2)	679±240	659±197	698±233	678±243	675±234	694±229	661±195	752
	A_{sp} (%)	5.9±3.5	6.1±1.5	5.3±2.9	6.2±4.4	5.9±3.4	5.6±3.6	5.7±0.7	5.9
	SIR_{loss} (W/m^2)	38±18	44±17	37±17	39±22	39±18	38±21	42±14	48

Origin of the Variability

First only *SZA* and F_{ESD} are left variable (Table 3, data set d2). The main consequence is to get closer to the annual average than with the data set d1. The variability of both *SZA* and F_{ESD} have a great influence on *DNI* which is reduced by 98 W/m^2, and a little influence on A_{sp} which is reduced by 0.2%. SIR_{loss} is also reduced by 6 W/m^2. Moreover, the *SZA* variability generates only 0.7% standard deviation on A_{sp}, but 209 W/m^2 on *DNI* (with F_{ESD}). Eventually, the standard deviation on SIR_{loss} is slightly smaller than the standard deviation with all variable parameters. Second, *AOT* is also made variable (d3). On the contrary to *SZA* and F_{ESD} variabilities, the *AOT* variability increases *DNI*. *DNI* becomes larger than the annual average, and A_{sp} remains close to the annual average. SIR_{loss} becomes equal to the annual average. Expectedly, the standard deviation increases to become almost equal to the standard deviation with full variability. Most variability of SIR_{loss} is generated by the variability in *SZA*, while most variability of A_{sp} is generated by the variability in *AOT*.

Eventually, computations are made by assuming that only one of the four atmospheric parameters is constant along the year (d4-d7). The variability of *WVC* has little influence on the solar resource parameters, and *SIR* would be under estimated by only 4 W/m^2. However, a constant value of *ALH* of 3.3 km significantly increases A_{sp}, from 5.9 to 6.2%. Indeed, no more compensation occurs between *AOT* and *ALH* changes. In particular, in summer, A_{sp} would increase with *ALH* of 3.3 km instead of 4.3 km. Consequently the standard deviation also significantly increases. As *DNI* is not affected, SIR_{loss} is also over estimated, but by only 1 W/m^2, and *SIR* is eventually little affected.

The variabilities of *AOT* and the Ångström exponent also significantly affect the solar resource parameters. A constant value of *AOT* significantly over estimates SIR_{loss}, and under estimates *SIR* by 20 W/m^2 (-3%), and a constant value of the Ångström exponent significantly under estimates A_{sp}, and over estimates *SIR* by 19 W/m^2 (+3%).

CONCLUSION

We made a sensitivity study of the solar irradiance incident on the receiver (SIR) of a solar tower plant (STP), which does not only depend on the direct normal irradiance (DNI) but also on the atmospheric transmittance between the heliostat and the receiver. Four solar resource parameters are identified, *DNI*, *SIR*, the slant path attenuation (A_{sp}) and the solar irradiance lost along the slant path (SIR_{loss}). We studied their dependence on four atmospheric parameters, which are the aerosol optical thickness (AOT), the Ångström exponent, the aerosol layer height (ALH), the water vapour content (WVC), and the solar zenith angle (SZA). First, we made computations for variable typical atmospheric conditions affected by desert dust events, demonstrating the seasonal influence of the solar resource. Then, we made an application on data acquired during one year by AERONET at Ouarzazate. The origin of the

variability of the solar resource estimates is studied by setting each of the atmospheric parameter to the constant value of the annual average.

A_{sp} and SIR_{loss} are highly dependent on *AOT* and *ALH*. A_{sp} varies by a factor of 2 from *AOT* of 0.10 to 0.30-0.40, and by a factor of 4 to *AOT* of 0.60-0.90, depending on the other parameters. SIR_{loss} is less dependent on *AOT* because of compensating changes in A_{sp} and *DNI*, and it varies by less than a factor of 3. For a change of *ALH* by a factor of 3, A_{sp} and SIR_{loss} vary by a factor of ~2. SIR_{loss} is also affected by *SZA* and it shows a daily cycle similar to *DNI* with null values during the night and a maximum reached at noon. All parameters are also affected by the Ångström exponent.

The sensitivity study shows that the variability in the three aerosol parameters have to be considered to estimate the solar resource in a STP. For example, despite a factor of 10 in *AOT* between typical summer and winter conditions at Ouarzazate, A_{sp} varies by a factor of only 2.7 and SIR_{loss} by a factor of only 1.9. Several atmospheric parameters are indeed correlated, as *AOT* and *ALH* both increasing simultaneously at Ouarzazate. This is why the standard deviation of A_{sp} on one year at Ouarzazate is only 3.5% (for an average of 5.9%) despite 100% standard deviation on observed *AOT*. The variability of *ALH* affects significantly the annual average of A_{sp}, and both *AOT* and the Ångström exponent can not be set constant as their variability each affects *SIR* up to 3%, by changing both *DNI* and A_{sp}. It is also important to make computations at the finest time resolution. *SIR* is indeed much larger when computed with mean annual input parameters than when computed at the hourly resolution.

It is important to compute simultaneously *DNI*, A_{sp} and *SIR*. Indeed, the mean annual SIR_{loss} is not equal to the product of the mean annual *DNI* and the mean A_{sp}. Moreover radiative transfer needs to be fully resolved not only in the atmosphere above the STP but also interacting with the heliostat field and the ground environment. Here, the slant path attenuation was studied by applying the approximation of strict *DNI* [8], while full radiative transfer would estimate not only the slant path attenuation loss, but also the other optical losses, and even gains by atmospheric scattering [20], similar to the circumsolar contribution to *DNI* [8].

The high sensitivity to the atmospheric parameters also implies to make computations for several years, as inter annual changes can be significant. Consequently, we may need to compute the solar resource parameters with global data sets generated by satellite observation (e.g. MODIS) and by assimilation (e.g. MACC) which extend over more than ten years. However, biases with local conditions may significantly affect the solar resource estimates. It is consequently necessary to assess the validity of such global data sets for local conditions representative of any STP, including the cloud cover influence.

ACKNOWLEDGMENTS

All data providers are gratefully acknowledged: AERONET PIs for aerosol and water vapor information and ECMWF for the boundary layer height.

REFERENCES

1. L. Li, J. Coventry; Bader, R.; Pye, J. and W. Lipiński, Opt. Express OSA **24**, A985-A1007 (2016).
2. J. Polo, J. Ballestrín, J. Alonso-Montesinos, G. López-Rodriguez; Barbero, J.; Carra, E.; Fernández-Reche, J.; Bosch, J. L. and F. J. Batlles, Solar Energy **157**, 803 - 810 (2017).
3. C. A. Gueymard, Solar Energy **86**, 3544 - 3553 (2012).
4. T. Elias, D. Ramon, L. Dubus, C. Bourdil, E. Cuevas-Agulló, T. Zaidouni, P. Formenti, AIP Conference Proceedings, 1734 (2016) 150004, doi: 10.1063/1.4949236.
5. J. Polo, J. Ballestrin, E. Carra, Solar Energy, 134, 219-227 (2016).
6. B. N. Holben, et al., Rem. Sens. Environ. **66**, 1-16 (1998).
7. T. Elias, D. Ramon, M. A. Garnero, L. Dubus, C. Bourdil, AIP Conference Proceedings, 1850 (2017) 140005
8. P. Blanc, Espinar, B., Geuder, N., Gueymard, C., Meyer, R., Pitz-Paal, R., Reinhardt, B., Renné, D., Sengupta, M., Wald, L. and Wilbert, S., Solar Energy **110**, 561 – 577 (2014).
9. B. A. Bodhaine, Wood, N. B., Dutton, E. G., and J. R. Slusser, J. Atm. Ocean Technol. **16**, 1854–1861 (1999).
10. K. Bogumil, J. Orphal, Voigt, S., Spietz, P., Fleischmann, O. C., Vogel, A., Hartmann, M., Kromminga, H., Bovensmann, H., and J. P. Burrows, J. Photochem. and Photobio. A: Chem. **157**, 167–184, (2003).
11. Kato, S.; Ackerman, T. P.; Mather, J. H. and E. E. Clothiaux, Journal of Quantitative Spectroscopy and Radiative Transfer **62**, 109 - 121 (1999).

12. G. Anderson, Clough, S., Kneizys, F., Chetwynd, J., and Shettle, E., Tech. Rep. AFGL-TR-86-0110, Air Force Geophys. Lab., Hanscom Air Force Base, Bedford, Mass. (1986).
13. R. Kurucz, Synthetic infrared spectra, in: Proceedings of the 154th Symposium of the International Astronomical Union (IAU); Tucson, Arizona, March 2-6, 1992, Kluwer, Acad., Norwell, MA (1992).
14. C. A. Gueymard, Solar Energy **74**, 355-379 (2003).
15. M. Hess, P. Koepke, and I. Schult, Bulletin of the American Meteorological Society **79**, 831–844, (1998).
16. D. P. Dee, S. M. Uppala, A. J. Simmons, P. Berrisford, Q.J.R. Meteorol. Soc., 137: 553-597 (2011)
17. C. Gueymard, Journal of Solar Energy Energineering **133**, 031024 (2011).
18. G. López, C. A. Gueymard; Bosch, J. L.; Rapp-Arrarás, I.; Alonso-Montesinos, J.; Pulido-Calvo, I.; Ballestrín, J.; Polo, J. and J. Barbero, Solar Energy **169**, 34 – 39 (2018).
19. C. Gueymard, G. Lopez, I. Rapp-Arraras, AIP conference proceedings **1850**, 140010 (2017).
20. M. Moulana, T. Elias, C. Cornet, D. Ramon, SolarPaces 2018 (2019).